Comparison of natural and anthropogenic nutrient sources in the Southern California Bight

Meredith D.A. Howard, Martha Sutula, David Caron[1], Yi Chao[2], John D. Farrara[2], Hartmut Frenzel[3], Burton Jones[1**], George Robertson[4], Karen McLaughlin and Ashmita Sengupta*

Abstract

Eutrophication of coastal waters has greatly increased in the last several decades throughout the world, with demonstrated linkages to anthropogenic nutrient loads. Anthropogenic inputs been shown to provide significant sources of nitrogen that have been linked to increased primary production and are considered the most significant factor contributing to the global increase in harmful algal blooms (HABs). While a growing number of studies have suggested a linkage between anthropogenic nitrogen sources and HABs in California, there is a general perception that in upwelling regions, such as California, the flux of anthropogenic nutrient inputs are small relative to upwelling flux, and therefore they have relatively little effect on the productivity of coastal waters. However, no studies to date have quantified the natural and anthropogenic inputs on regional and local scales in the SCB to verify the accuracy of this perception. In order to test the hypothesis that natural sources (e.g., upwelling) greatly exceed anthropogenic nutrient sources to the SCB, this study compared the contributions of nitrogen (N) from four major nutrient sources: 1) upwelling, 2) treated wastewater effluent discharged to ocean outfalls, 3) riverine runoff, and 4) atmospheric deposition. This comparison was made using large regional datasets combined with modeling on both regional (SCB-wide) and sub-regional scales. The results from this study show that at the regional bight-wide spatial scale, upwelling is the largest source of nitrogen by an order of magnitude to effluent and two to riverine runoff. However, at smaller spatial scales, natural and anthropogenic contributions were equivalent. In particular, wastewater effluent and upwelling contributed the same quantity of nitrogen in several regions of the SCB. These findings contradict the currently held perception that in upwelling-dominated marine ecosystems, anthropogenic nutrient inputs are negligible and are consistent with the growing number of studies that have suggested a linkage between anthropogenic nitrogen sources and HABs in California nearshore waters. These results of this study suggest that anthropogenic

[1]University of Southern California, Department of Biological Sciences, Los Angeles, CA

[2]California Institute of Technology, Jet Propulsion Laboratory, Pasadena, CA

[3]University of California, Department of Atmospheric and Oceanic Sciences, Los Angeles, CA

[4]Orange County Sanitation District, Fountain Valley, CA

[*]Present Address: Remote Sensing Solutions, Inc., Pasadena, CA

[**]Present Address: King Abdullah University of Science and Technology, Thuwal, Kingdom of Saudi Arabia

nutrients cannot be dismissed as a significant source of nutrients for algal blooms in the SCB.

Introduction

Eutrophication of coastal waters, the accelerated accumulation of organic matter from an overabundance of algae (Nixon 1995), has greatly increased in the last several decades throughout the world, with demonstrated linkages to anthropogenic nutrient loads (see reviews Howarth *et al.* 2002a,b, 2008; Paerl and Piehler 2008). Human population growth (resulting in increased sewage discharges), development of coastal watersheds, agricultural and aquaculture runoff into the coastal oceans, and burning of fossil fuels are among the many factors contributing to increased eutrophication of coastal waters (Anderson *et al.* 2002, Howarth 2008). Anthropogenic inputs of agricultural runoff, wastewater and sewage discharge, and groundwater discharge have all been shown to provide significant sources of nitrogen that have been linked to increased primary production and/or harmful algal blooms (HABs; Lapointe 1997, 2004, 2005a,b; Glibert *et al.* 2005a, 2006; Anderson *et al.* 2002, 2008; Heisler *et al.* 2008). Anthropogenic nutrient inputs are considered the most significant factor contributing to the global increase in the frequency and intensity of harmful algal blooms (HABs; Smayda 1990; Anderson *et al.* 2002, 2008; Howarth *et al.* 2002; Hallegraeff 2004; Glibert *et al.* 2005a,b; GEOHAB 2006; Glibert *et al.* 2006; Heisler *et al.* 2008). While many studies have focused on agricultural runoff, wastewater has also been found to promote HABs and increase primary productivity; in some regions, wastewater has been shown to be more important than upwelling as a nitrogen source (Chisholm *et al.* 1997; Lapointe 1997; Jaubert *et al.* 2003; Thompson and Waite 2003; Lapointe *et al.* 2004, 2005b).

Nitrogen has been the focus of most coastal eutrophication studies because it has been shown to be the primary limiting macronutrient for algae in coastal waters and in California (Dugdale 1967; Ryther and Dunstan 1971; Eppley *et al.* 1979; Nixon 1986, 1995; Kudela and Dugdale 2000). However, recent research has shown that the nitrogen form, not just quantity, is important for HABs and algal blooms (Glibert *et al.* 2006, Howard *et al.* 2007, Switzer 2008, Kudela *et al.* 2008, Cochlan *et al.* 2008).

Within the SCB, recent studies have shown that algal bloom intensity has increased over the last decade, with chronic blooms documented in areas of the SCB that have significant anthropogenic nutrient inputs (Nezlin *et al.* 2012). Prior to 2000, toxic outbreaks of *Pseudo-nitzschia* (an algal diatom that produces domoic acid) were considered rare (Lange *et al.* 1994); however, in recent years, frequent occurrences and high concentrations of this toxin have been documented in the SCB (Trainer *et al.* 2000, Busse *et al.* 2006, Schnetzer *et al.* 2007, Caron *et al.* 2010, Caron unpublished data). Increased awareness of toxic HAB events served as the primary motivation for establishment of the Harmful Algae and Red Tide Regional Monitoring Program by the Southern California Coastal Ocean Observing System (SCCOOS). This ongoing program collects weekly HAB species and toxin information from five pier locations in Southern California (data available online, http://www.sccoos.org/data/habs/index.php).

There is a general perception that in upwelling regions, such as California, the flux of anthropogenic nutrient inputs are small relative to upwelling flux, and therefore they have relatively little effect on the productivity of coastal waters. Upwelling is the process by which vertical currents transport deep nutrient-rich water to the surface displacing nutrient-depleted surface water. No studies to date have quantified the natural and anthropogenic inputs on regional and local scales in the SCB to verify the accuracy of this perception. However, a growing number of studies have suggested a linkage between anthropogenic nitrogen sources and HABs in California, particularly with regard to anthropogenically-influenced riverine runoff (Kudela and Cochlan 2000, Kudela and Chavez 2004, Beman *et al.* 2005, Kudela *et al.* 2008). Additionally, physiological studies have shown several common California HAB species are capable of utilizing anthropogenic nitrogen forms, such as urea (Herndon and Cochlan 2007, Cochlan *et al.* 2008, Kudela *et al.* 2008) for growth and toxin production can be increased under these conditions (Howard *et al.* 2007).

In order to test the hypothesis that natural sources (e.g., upwelling) greatly exceed anthropogenic nutrient sources to the SCB, this study compared the contributions of nitrogen (N) from four major nutrient sources: 1) upwelling, 2) treated wastewater effluent discharged to ocean outfalls, 3) riverine runoff, and 4) atmospheric deposition. This comparison was made using large regional datasets combined with modeling on both regional (SCB-wide) and sub-regional scales. This is the first study to make this comparison on the United States west coast.

Methods

Study Area

The SCB lies along the southern part of the Pacific coast of the continental United States. The continental coastline generally runs along a north south gradient beginning at Cape Flattery, Washington (~48° 23'N), until Cape Mendocino in northern California (~40° 15'N), then turns toward a south-southeast direction. The continuum is broken by a bend or curvature in the coastline between Point Conception (~34° 34'N) and the Mexico international border (~32° 32'N). The SCB includes an ocean area of 78,000 km^2 (Dailey *et al.* 1993) and numerous islands offshore. The bottom topography consists of submarine mountains and valleys, neither of which could be considered a classical continental shelf nor a classical continental slope.

A ring of coastal mountain ranges defines southern California (SC). The mountain ranges shelter the coastal area from dominating northwesterly winds and create a "coastal basin" where cool, dense air is trapped, resulting in much weaker wind and sea patterns than over the open ocean (Dorman and Winant 1995). Southern California's climate exhibits a relatively dry summer and wet winter season. During the dry season a semi-permanent eastern Pacific high-pressure area dominates SC. The marine layer is a prominent feature from late spring through early fall. Beginning late fall to early spring (October through March) the high-pressure ridge gets displaced and the southern margin of the polar jet stream affects SC. The probability of rain increases because the marine layer is not dominant anymore and subtropical moisture occasionally feeds cold fronts crossing the SC area from Pacific storms. Over 90% of the precipitation generally occurs during this time period. The migratory nature of the region's storm fronts causes alternating periods of dry and wet weather during the rainy season.

The ocean region within the SCB is dominated by the equatorward California Current (CC). The CC is a typical broad eastern boundary current (Hickey 1979, Lynn and Simpson 1987) that transports cold Subarctic water from north to south throughout the year along a typically narrow (3 to 6 km) coastal continental shelf. The CC is not steady but migrates seasonally onshore and offshore, producing a rich eddy field (Burkov and Pavlova 1980, Strub and James 2000, Haney *et al.* 2001). As the CC passes Point Conception, it turns south-southeast along SC's outer continental slope, then a portion branches (~32°N) eastward to northward along the coast (Hickey 1992, Harms and Winant 1998, Bray *et al.* 1999), forming a large gyre known as the Southern California Eddy (Figure 1). The poleward current along the coast is called the Southern California Countercurrent (Sverdrup and Fleming 1941). It transports warm southern water into Santa Monica Bay and the Santa Barbara Channel.

Surface current flows may not reflect sub-pycnocline currents (Hamilton *et al.* 2006). During spring, the intensity of the equatorward CC increases compared to the poleward Southern California Countercurrent. Its jet migrates onshore, and the eastward branches penetrate into the Southern California Bight through the Santa Barbara Channel and onward south of the Channel Islands (Reid and Mantyla 1976, Hickey 1979, Bray *et al.* 1999). The islands act as barriers to deflect surface currents in different directions. Near shore, over the continental shelf and borderland slope, the near surface flow is commonly equatorward while the California Undercurrent is poleward (Hickey 1993). Figure 1 shows the circulation patterns in the SCB.

Study Approach: Estimation and Comparison of Nutrient Sources

The nitrogen (N) fluxes to the SCB were estimated for upwelling, wastewater effluent discharge, riverine runoff, and atmospheric deposition. A combination of field measurements and modeling targeted over a one-year period (January-December 2010) was used to estimate the contribution of each nutrient source on a bight-wide scale as well as for six smaller sub-regional areas including: Santa

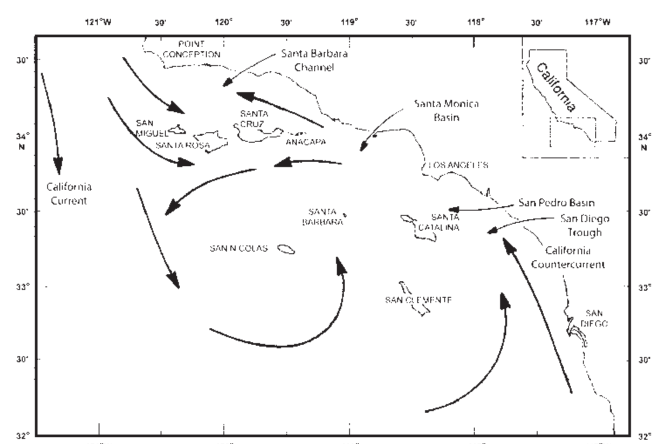

Figure 1. The circulation patterns in the SCB (adapted from Hickey 1992).

Barbara (2,405 km^2), Ventura (1,449 km^2), Santa Monica Bay (1,571 km^2), San Pedro (1,641 km^2), North San Diego (1,837 km^2), and San Diego (1,020 km^2). The combined area of all of the sub-regions makes up 20% of the total bight-wide area of the SCB. Figure 2 shows the bight-wide area (dashed line) and the six sub-regions (black lines). Nutrient inputs were estimated as annual loads for the bight-wide scale and are reported in kg N yr^{-1}. Annual fluxes were calculated for the six sub-regional areas in order to compare sub-regions that vary in spatial area and are reported as kg N km^{-2} yr^{-1}.

Modeling to Estimate Upwelling

The upwelling contribution of N was estimated using the Regional Oceanic Modeling System (ROMS), a three-dimensional ocean circulation model for the US West Coast (Marchesiello *et al.* 2003), was coupled with an NPZD-type ecosystem-biogeochemistry model (Gruber *et al.* 2006) to generate a reanalysis of the ocean environment from January to December 2010. This model integration resulted in highly time-resolved output of the three dimensional physical and biogeochemical parameters. The ROMS model saves output of the daily averages of all advection terms in Equation 1 (Gruber *et al.* 2006) and the output was integrated over time and space.

$$\frac{\partial B}{\partial t} = \nabla \cdot K \nabla B - \vec{u} \cdot \nabla_h B - (w + w^{\text{sink}}) \frac{\partial B}{\partial z} + J(B) \qquad \text{Eq. 1}$$

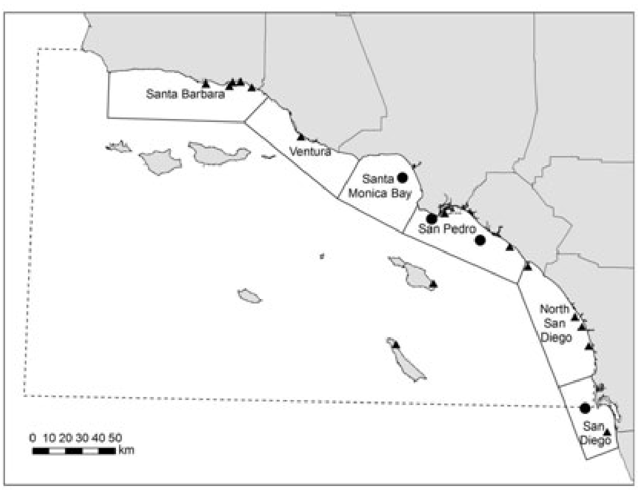

Figure 2. Regional and sub-regional SCB boundaries used to calculate fluxes of each of the four major sources. The area used for regional estimates is outlined with a dashed line; sub-regions are labeled and outlined with solid black line.

where K is the eddy kinematic diffusivity tensor, and where ∇ and ∇_h are the 3-D and horizontal gradient operators, respectively. The horizontal and vertical velocities of the fluid are represented by $\vec{u}$ and w, respectively. The w^{sink} represents the vertical sinking rate of the biogeochemical components and $J(B)$ represents the source minus sink term.

All of these terms are described in detail in Gruber *et al.* 2006. From this detailed output, periods of upwelling were determined using vertical velocity, lateral advection, and temperature fields, and then the net mass of nitrate and ammonium from lateral and vertical fluxes to the euphotic zone was calculated. The total vertical flux assimilated by the model includes advection and diffusion while the total lateral flux was assimilated for advection only. Daily estimates were summed to provide an annual estimate. The TN (ammonium and nitrate) estimates were made over a range of spatial scales, from a Bight-wide scale (Figure 2 dashed line) to smaller sub-regional scales (Figure 2 solid black line).

Model Description

ROMS is a free-surface, hydrostatic, three-dimensional primitive equation regional ocean model (Marchesiello *et al.* 2001; Shchepetkin and McWilliams 2005, 2006). A description and validation of the ROMS model at the 15-km spatial scale has been published (Gruber *et al.* 2006). This ROMS 3-D model provides both existing "nowcast" and predictive "forecast" assimilations (up to 48 hours in 6-hour increments) of satellite sea surface temperature, HF radar surface current, subsurface temperature, and salinity profiled from Argo floats and gliders. The ROMS output (for the physics-only model runs) is provided at both the JPL ROMS web site (http://ourocean.jpl.nasa.gov/SCB) and the SCCOOS web site (www.sccoos.org/data/roms).

The ROMS configuration used consists of a single domain covering the southern California coastal ocean from Santa Barbara to San Diego at a resolution of 1 km. With respect to the model grid, the vertical discretization uses a stretched terrain-following coordinate (S-coordinate) on a staggered grid over variable topography (Song and Haidvogel 1994). The stretched coordinate allows increased resolution in areas of interest, such as the thermocline and bottom boundary layers. ROMS uses a sigma-type vertical coordinate in which coordinate surfaces follow the bottom topography. In the SCB configuration, there are 40 unevenly-spaced sigma surfaces used with the majority of these clustered near the surface to better resolve processes in the mixed layer. The horizontal discretization uses a boundary-fitted, orthogonal curvilinear formulation. Coastal boundaries are specified as a finite-discretized grid via land/sea masking. The SCB configuration of ROMS has been tested and used extensively (Dong *et al.* 2009).

Boundary conditions for the SCB domain are provided from a separate data-assimilating ROMS domain that covers the entire coast of California and northern Baja California at a resolution of 3 km. The tidal forcing is added through lateral boundary conditions that are obtained from a global barotropic tidal model (TPXO.6; Egbert *et al.* 1994, Egbert and Erofeeva 2002) which has a horizontal resolution of 0.25 degrees and uses an inverse modeling technique to assimilate satellite altimetry cross-over observations. Eight major tide constituents at the diurnal and semidiurnal frequencies (M2, K1, O1, S2, N2, P1, K2 and Q1) are used. The atmospheric forcing required by the ROMS model is derived from hourly output from forecasts performed with a regional atmospheric model, the Weather Research and Forecasting System (WRF). This model has been used in several studies in the SCB region (Conil and Hall 2006; Hughes *et al.* 2007, 2008). The horizontal resolution is 4 km and the lateral boundary forcing and initial conditions are derived from the NCEP NAM 12-km North American model daily 00GMT forecasts. The surface latent and sensible heat fluxes, as well as surface evaporation rates, are derived from WRF surface air temperatures, surface relative humidity, 10 m winds, solar/terrestrial radiation, and ROMS sea surface temperatures (SSTs), using the bulk formula proposed by Kondo (1975). The fresh water flux is computed as the calculated evaporation rate minus the WRF precipitation rate (E-P). The wind stress is derived from the 10 m winds using the formula of Large and Pond (1982). The variables used for computing the ocean model forcing have been evaluated against buoy data. The surface winds are satisfactorily accurate, with RMS errors of 2 to 3 m s^{-1} in speed and 30 degrees in direction. Comparison of modeled versus measured surface air temperatures and relative humidity show good accuracy with errors of 1 to 2^{o}C and 5 to 10%.

The biogeochemical model that was used in this ROMS configuration is a Nutrient-Phytoplankton-Zooplankton-Detritus (NPZD) model based on Fasham *et al.* (1990). The model was optimized and validated for the US West Coast coastal upwelling region by Gruber *et al.* (2006). This model has been validated and gives good results in the upwelling dominated coastal zone, but it fails to reproduce observations further offshore in more nutrient-depleted areas (Gruber *et al.* 2006). A full description of the model can be found in Gruber *et al.* (2006), but is described briefly here.

The NPZD model includes a single limiting nutrient (nitrogen) and a diatom-like single phytoplankton class. While the model output was only used to calculate nitrate and ammonium lateral and vertical fluxes, a total of twelve state variables are tracked including: nitrate, ammonium, phytoplankton, zooplankton, small and large detritus (both nitrogen and carbon concentrations due to varying C:N ratios), oxygen, dissolved inorganic carbon, calcium carbonate, and total alkalinity. The chlorophyll:carbon ratio in phytoplankton and the organic nitrogen and carbon matter content of the sediment are carried as state variables. The sinking of all particulate pools (i.e., phytoplankton and detritus) is modeled explicitly. Only two parameters were changed from Gruber *et al.* 2006): the initial slope of the light-response curve for phytoplankton growth and the mortality rate of phytoplankton were both doubled to improve the resulting net primary productivity (Gruber *et al.* 2011).

In the absence of a larger domain model with the same NPZD biogeochemical model characteristics, biogeochemical boundary conditions were based on the physical boundary conditions, modeled at daily time steps, and the relationship between physical quantities (either temperature or potential density) and nutrients like nitrate was used to derive initial and boundary conditions for nitrate (NO_3) and ammonium (NH_4), as summarized in Table 1. Initial and boundary conditions for nitrate concentrations were forced with a polynomial regression that describes the relationship between NO_3 and density (σ_Θ), defined for the SCB from temperature, salinity, and nitrate data from the World Ocean Atlas 2005 (Garcia *et al.* 2006; Figure 3).

Because there were no observed data available for ammonium (NH_4), climatological biogeochemical boundary and initial conditions were used to determine a relationship between potential density and NH_4. As Figure 3 shows, the scatter is much larger for this relationship than for NO_3.

Table 1. List of polynomial parameters for the biogeochemical boundary conditions in ascending order, e.g., $NO_3(\sigma_\Theta>26.8) = -20258 + 1484.7*\sigma_\Theta + -27.1422*\sigma^2$.

Variable	σ_Θ Range 1	Polyn. 1	σ_Θ Range 2	Polyn. 2	σ_Θ Range 3	Polyn. 3
Nitrate	Up to 24.99	-48.0343 1.9910	25.0 .. 26.79	-371.8125 11.3264 0.1449	Over 26.8	-20258.0000 1484.7000 -27.1422
Chl-a (top 50 m)	All values	-547.1559 42.7240 -0.8334	n/a	n/a	n/a	n/a
Chl-a (> 50 m)	All values	17.4953 -0.7332	n/a	n/a	n/a	n/a
Ammonium	Up to 24.82	-1.9986 0.0866	24.82 .. 26.42	-265.6287 20.7761 -0.4056	26.42 .. 27.2	170.326 -12.5235 0.2302

Wastewater Effluent Discharge

Nutrient loads from wastewater effluent discharged from outfalls to the SCB were estimated for both large (>100 MGD) and small (<25 MGD) Publicly Owned Treatment Works (POTWs) in each sub-region (Table 2). A greater emphasis was placed on measuring nutrient concentrations in wastewater effluents from large POTWs than from small POTWs because large facilities represent 90% of the total POTW discharges to the SCB via ocean outfalls (Lyon and Stein 2008). Large POTW nutrient loads were determined by quarterly measurements of nutrient concentrations from December 2008 through December 2009; these quarterly concentrations were combined with monthly discharge flows from 2010 NDPES monitoring reports from each of the large POTW facilities. Samples were analyzed for total dissolved nitrogen (TN) following EPA method SM4500-N, nitrate following EPA 300.0 and SM4500, ammonia following method EPA 350.1 and SM4500 and urea using Goeyens *et al.* 1998. An inter-laboratory comparison was conducted for these analytes and the variability was determined to be negligible.

The small POTW nutrient loads were determined using available data published for 2005 (Lyon and Stein 2008). Effluent nutrient concentration data for small POTWs relied on existing data from NDPES monitoring reports for 2005 (Lyon and Stein 2008). Small POTW effluent concentration data were compiled for the following nutrient forms: nitrate+nitrite (NO_X), ammonia (NH_3), total dissolved nitrogen (TN) and organic nitrogen where available.

POTW N load (bight-wide) was estimated by multiplying nutrient concentrations (mg L^{-1}) with annual flow volume (L) and POTW N fluxes for each sub-region were estimated by dividing the N load by the area (km^{-2}) of that sub-region.

Riverine Loads

Riverine nutrient loads to the SCB were estimated using empirical wet- and dry-weather data for monitored watersheds in combination with modeled wet-weather loads for unmonitored watersheds for the period of October 2008 to December 2010. Methodology and discussion of results are presented in detail in Sengupta *et al. In Review*, but summarized here.

Field Data Collection

Discharge and water quality samples were collected at 34 wet weather and 57 dry weather mass emission stations by Ventura, Los Angeles, Orange, and San Diego Counties under their National Pollution Discharge Elimination System (NPDES) permits or by SCB Regional Monitoring Program partners during the period of November 2007-October 2010. Sengupta *et al.* (*In Review*) provides details on the methods used and a summary of the wet- and dry-weather monitoring and the 38 mass loading stations utilized for the study.

Modeling Methods

A spreadsheet model based on the Rational Method (O'Loughlin *et al.* 1996) was used to generate freshwater runoff Q (m^3 day^{-1}) and the nutrient

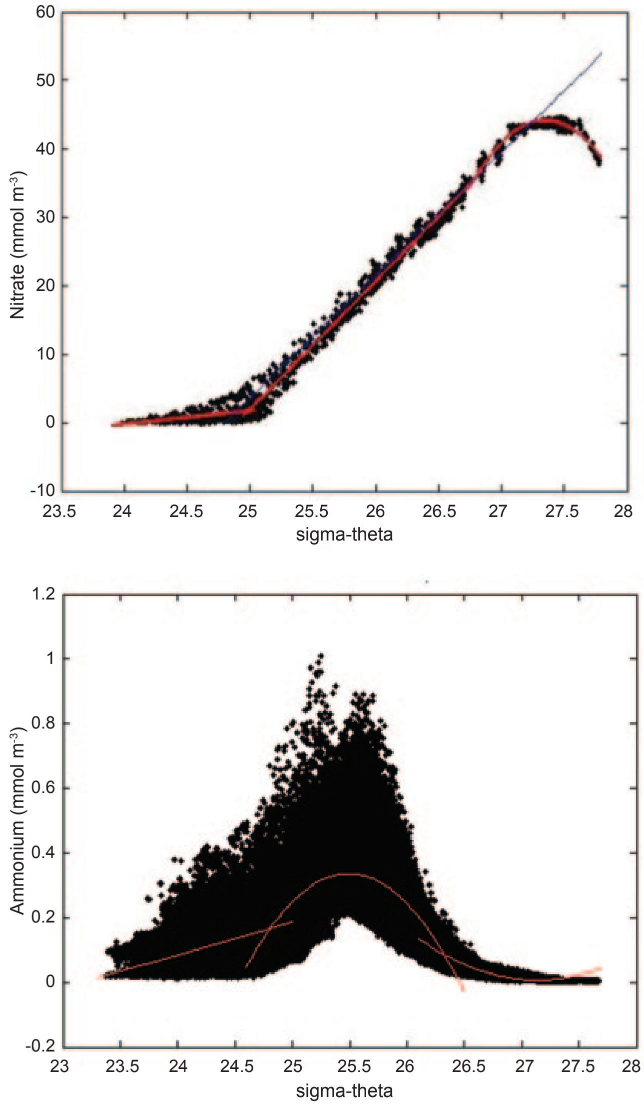

Figure 3. Relationship between potential density (sigma-theta) and nitrate (top) and ammonium (bottom) in the Southern California Bight. Nitrate and ammonium data (black dots) are derived from the World Ocean Atlas (2005) and ROMS tests run with climatological boundary conditions, respectively. Red lines designate the step-wise polynomial fits.

loads (N and P) associated with wet weather events. Modeled storm discharge (Q) was calculated as a function of drainage area (A, km^2), mean rainfall intensity (I, mm day^{-1}), hydraulic runoff coefficient (C), and conversion constant (k):

$$Q = A\ I\ C\ k \qquad \text{Eq. 2}$$

Hydraulic runoff coefficient (C) varied as a function of land use/cover type (Sengupta *et al. In Review*). The Ackerman and Schiff model (2003) was improved by refining land use-specific runoff concentrations for NOx and NH_4, based on previously published values from recently published studies (Stein *et al.* 2007, Yoon and Stein 2008) and TN runoff concentrations were derived from empirical data for this study (Sengupta *et al. In Review*).

Within each watershed, total discharge (Q) was then calculated as the sum of discharge associated with six land use categories: agriculture, commercial, industrial, open space (natural), residential, and other urban. The daily nutrient loads were estimated as the sum of the product of the runoff concentration (c) and Q for each land use, using Equation 2.

The drainage area (A) is delineated for each watershed based on hydraulic unit code (HUC) Boundaries. The model domain includes all southern California coastal watersheds in San Diego, Orange, Riverside, Los Angeles, San Bernardino, Ventura and Santa Barbara counties with an initial total watershed area of 27,380 km^2. Watershed areas larger than 52 km^2 upstream of dams were excluded in the model domain, in order to mimic the retention of water by dams (Ackerman and Schiff 2003). The final model domain comprised of 98 watersheds with a total area of 14,652 km^2. Each of the watersheds was populated with land cover data from Stein *et al.* (2007), and aggregated into the six land use categories.

Daily precipitation data for approximately 200 rain gauge stations were obtained from the National Oceanic and Atmospheric Administration (NOAA), National Environmental Satellite, Data and Information Service (NESDIS), National Climatic Data Center (NCDC) and Climate Data Online (CDO) database. Data from the 200 rain gauge stations were transformed to estimate mean precipitation over the 98 watersheds relevant to the study. Precipitation data was interpolated within each watershed on a regular grid using a Biharmonic Spline Interpolation method (Sandwell 1987).

To estimate the anthropogenic influence on nutrient fluxes to the SCB, a model scenario with 100% open space land-use for the entire Bight, representing a "pre-urbanization" baseline, was run. Because there were no dams withholding potential runoff in the modeled pre-urbanized state, the model domain was expanded to include areas above existing dams. Rainfall data was not available for the period representing the pre-urbanized state; therefore, current rainfall data (2008-2009) were used to estimate loads. This enables a comparison of pre- and post-urbanization loads without any bias due to differences in precipitation.

Table 2. Location and relative size of POTWs used for effluent discharge load estimates by sub-region. S= Small; L = Large.

Sub-region	POTW Name	Size	GPS Coordinates (Latitude/Longitude)
Santa Barbara	Goleta WWTP	S	34.401667/-119.824167
	El Estero WWTP	S	34.391944/-119.668889
	Montecito WWTP	S	34.413333/-119.647778
	Summerland WWTP	S	34.416663/-119.596671
	Carpinteria WWTP	S	34.388333/-119.521654
Ventura	Oxnard WWTP	S	34.126111/-119.190556
Santa Monica Bay	Hyperion Treatment Plant	L	33.911967/-118.52145
San Pedro	Joint Water Pollution Control Plant	L	33.695/-118.327361
	Treatment Plant No. 2	L	33.576667/-118.01
	Terminal Island WWTP	S	33.722111/-118.243389
	Aliso Creek Ocean Outfall	S	33.542778/-117.817222
North San Diego	San Juan Creek Ocean Outfall	S	33.436111/-117.698056
	Oceanside WWTP	S	33.162778/-117.391389
	Camp Pendleton WWTP	S	33.162778/-117.391389
	Fallbrook Public Utility District WWTP	S	33.162778/-117.391389
	Encina Ocean Outfall	S	33.109331/-117.347992
	San Elijo Water Pollution Control Facility	S	33.005833/-117.3025
San Diego	Point Loma WWTP	L	32.665278/-117.323611
	Hale Ave. Resource Recovery Facility	S	32.5375/-117.183333
	South Bay Water Reclamation Plant	S	32.5375/-117.183333
	International WWTP	S	32.5375/-117.183333

Atmospheric Deposition

Limited data are available on rates of atmospheric deposition of N to the SCB. Existing federal networks for estimation of atmospheric deposition (e.g., National Atmospheric Deposition Program; NADP) are focused on land-based wet deposition of nutrients. However, in Southern California, where rainfall typically occurs only 10 to 30 days per year, dry weather can potentially be more important to algal productivity in the Bight nearshore waters than wet deposition (Sabin and Schiff 2008). Therefore, dry-deposition sampling was conducted and wet deposition rates were calculated from existing data as described below.

Because available resources for this component were not sufficient to undertake ocean-based measurements of atmospheric deposition, atmospheric load calculations for the nearshore zone (at sub-regional scale, up to 20 km offshore) were derived from land-based estimates, although these estimates at a sub-regional scale likely represent an overestimate of loads. Atmospheric loads at the regional scale (Bight-wide) were not estimated due to lack of confidence in extrapolation of land-based estimates to areas >200 km offshore.

Dry Deposition

Several techniques using surrogate surfaces for estimating nitrogen dry deposition in semi-arid environments, including a water surface sampler and filter surfaces, been developed (Raymond *et al.* 2004, Moumen *et al.* 2004). Both of these techniques, used in the present study, use aerodynamic discs, are of short duration (2 - 4 days), and produce reproducible results when evaluated against the atmospheric concentrations and each other. Sampling for dry deposition was conducted three times over a six-month period at roof-top locations at the Hyperion Treatment Plant and the City of Oceanside Library. Samplers were deployed in duplicate for the water collector and triplicate for the filter collectors. Filter samplers were analyzed for NH_4 and NO_3, and water surface samplers were analyzed for NH_4 and NO_3. Concentrations were converted to a deposition rate by incorporating the surface area of the sampler and the duration of the sampling event (kg km^{-2} d^{-1}). The average deposition rate for the three sampling events was multiplied by the number of dry weather days during the January-December 2010 study year for a Bight-wide estimation of dry deposition. Results from the HTP site were applied to the Santa Monica Bay and San Pedro Bay sub-regions, and results from the Oceanside sampler were applied to all other sub-regions.

Wet Deposition

The wet deposition rates for the nitrogen and phosphorus estimates were calculated from the average annual rates for 2009 and 2010 at two NADP sites: Site 42, Los Angeles County (Tanbark Flat, 34.2071, -117.7618) and Site 94 San Bernardino County (Converse Flats, 34.1938, -116.9131). Wet deposition rates for NO_X and NH_4 from these two sites were averaged across sites and years, then applied as rate (kg km^{-2} d^{-1}) to the total number of wet days for the January-December 2010 study year.

Data Integration

All of the nutrient source estimates described above were converted into kg N yr^{-1} for the bight-wide source comparison and into kg N km^{-2} yr^{-1} for the sub-regional source comparison in order to compare sub-regions that vary in spatial area.

Error Analysis in TN and TP Loads

The error associated with the nitrogen and phosphorus loads was determined for the riverine runoff and effluent. Standard deviation of nutrient concentrations was multiplied by the total discharge (annual for effluent and wet or dry weather discharge respectively for the watershed). Total error was calculated as the square root of the squared sums of each of the individual estimates for each watershed, as given in Equation 3.

$$\text{Total Load Standard Deviation} = \left(\sum_1^{10}(C_e Q)^2\right)^{1/2} \quad \text{Eq. 3}$$

where C_e is the standard deviation in nutrient concentration for each watershed or large POTW effluent. Q is the total annual discharge (wet and dry calculated separately for riverine runoff).

The error was not calculated for the upwelling loads because the model is not yet fully validated at the spatial scale as used in this study (see "Uncertainty Associated with Nutrient Source Estimates" below).

Results

Bight-wide Regional Nitrogen and Phosphorus Loads

Total Nitrogen

At the SCB scale, TN loads differed by an order of magnitude with upwelling contributing the largest load and riverine runoff the smallest (Figure 4; Table 3). With respect to nutrient forms, upwelling consisted almost entirely of NOx (98.7%), with very little NH_4 (1.3%). Effluent loads consisted mostly of NH_4 (91.6%), with minor percentages of NOx (7.0%) and ON (1.0%). The riverine runoff was comprised mostly of NOx (60%) and ON (35%) with a smaller contribution from NH_4 (5%).

Estimates of Error

The error analysis of TN loads for the riverine runoff and effluent ranged from 3.3 to 23.7% for effluent and 2.4 to 37.8% for riverine runoff and are summarized in Table 4. The error was not calculated for the upwelling loads because the model is not yet fully validated at the spatial scale as it was used in this study (see "Uncertainty Associated with Nutrient Source Estimates" below).

Sub-Regional Nitrogen Fluxes

Total Nitrogen

Dominant TN sources varied by sub-region. For the three sub-regions with large POTW outfall discharges (Santa Monica Bay, San Pedro and San Diego), effluent and upwelling had similar annual

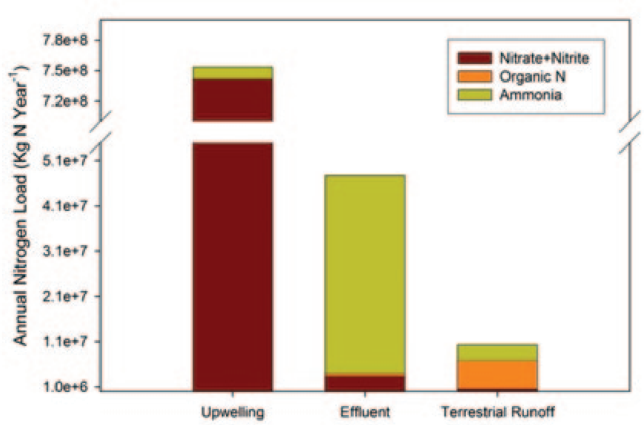

Figure 4. Annual total nitrogen loads (in MT N Year^{-1}) by source, with total nitrogen components separated into nitrate plus nitrite, organic nitrogen, and ammonia.

Table 3. **Bight-wide scale annual nitrogen loads for each nutrient source and constituent. All loads are in kg N year^{-1}. The percent of total nitrogen is listed in parenthesis.**

	Total Nitrogen	Nitrate + Nitrite	Ammonia	Organic N/Urea
Upwelling	7.5 x 10^8	7.4 x 10^8 (98.7)	1 x 10^7 (1.3)	NA
Effluent	4.8 x 10^7	3.4 x 10^6 (7)	4.4 x 10^7 (92)	5.0 x 10^5 (1)
Riverine Runoff*	1.0 x 10^7	3.5 x 10^6 (34)	6.0 x 10^5 (6)	6.2 x 10^6 (60)

*Data for January through October 2010.

TN fluxes (Figure 5; Table 5). These were 9.9 x 10^3 and 1.0 x 10^4 kg N km^{-2} yr^{-1} respectively for Santa Monica Bay, 1.3 x 10^4 and 2.4 x 10^4 kg N km^{-2} yr^{-1} respectively for San Pedro Bay and 7.6 x 10^3 and 2.4 x 10^3 kg N km^{-2} yr^{-1} for south San Diego region. Note that the upwelling flux estimated for San Diego is at the edge of the model boundary, therefore, it has a large amount of uncertainty. For these three regions, riverine runoff and atmospheric deposition were 1 to 2 orders of magnitude less than upwelling and effluent, respectively, with annual fluxes ranging from 1.4 x 10^2 to 6.0 x 10^3 kg N km^{-2} yr^{-1} for riverine runoff and 4.3 x 10^2 to 8.7 x 10^2 kg N km^{-2} yr^{-1} for atmospheric deposition.

The Santa Barbara and Ventura sub-regions were similar in that both had net annual downwelling rather than net upwelling, ranging from 1.0 x 10^5 to 2.1 x 10^4 kg N km^{-2} yr^{-1}, respectively. In these sub-regions, the major sources varied from effluent and atmospheric deposition in Santa Barbara (1.6 x 10^2 and 4.3 x 10^2 kg N km^{-2} yr^{-1} respectively) to roughly equivalent fluxes of effluent, riverine runoff and atmospheric deposition in Ventura (5.1 x 10^2, 1.4 x 10^2 and 8.7 x 10^2 kg N km^{-2} yr^{-1}, respectively). Only in North San Diego County was upwelling (3.7 x 10^4 kg N km^{-2} yr^{-1}) dominant by an order of magnitude over effluent (1.4 x 10^3 kg N km^{-2} yr^{-1}) and by two orders of magnitude over riverine runoff (6.0 x 10^2 kg N km^{-2} yr^{-1}) and atmospheric deposition (4.3 x 10^2 kg N km^{-2} yr^{-1}).

On average, riverine TN loads were 46% higher during storm events, which occur mostly from November to March, than during dry weather. During wet weather, eight watersheds (Los Angeles River, San Gabriel River, Calleguas Creek, San Diego Creek, Tijuana River, Santa Margarita River, Chollas Creek and Santa Ana River) account for 75% of the TN loads (Sengupta *et al. In Review*). The exception to the dominance of storm events to total annual loads was observed in San Gabriel, Los Angeles, and Santa Clara Rivers, where TN loads were comparable or greater during dry weather than during storm events. Thus the San Gabriel River, Los Angeles River, Santa Clara River, and Calleguas Creek watersheds represent the dry weather "hot spots" for nutrient loading to the SCB, representing 59 % of the dry weather total TN loads to the SCB (Sengupta *et al. In Review*). The flux of each nitrogen form is summarized in Table 6.

Table 4. Summary of the standard error calculated for nitrogen components of riverine runoff and effluent. Absolute and standard error reported in kg N year^{-1}.

Component	Riverine Runoff				Effluent	
	Wet Weather		Dry Weather			
	Absolute Error	% Error	Absolute error	% Error	Standard Error	% Error
TN	2.2 X 10^5	8.8	3.0 X 10^4	2.4	2.0 X 10^6	4.6
NO_3+NO_2	8.4 X 10^4	7.5	2.7 X 10^4	3.6	5.5 X 10^5	17.6
NH_4	9.4 X 10^4	37.8	8.1 X 10^3	11.6	1.3 X 10^6	3.3

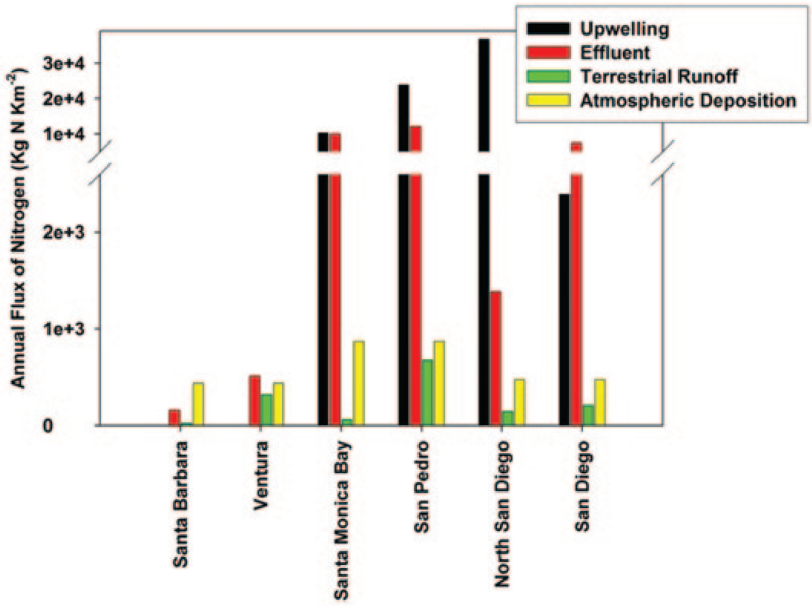

Figure 5. Annual nitrogen flux for upwelling, effluent , riverine runoff, and atmospheric deposition by sub-region.

Estimates of Contribution of Anthropogenic Activities to SCB Nutrient Loads

The contribution of anthropogenic activities to SCB nutrient loads were calculated based on changes in riverine loads from a pre-urbanization baseline, with the addition of effluent loads, all of which are assumed to be anthropogenic. No estimates of the anthropogenic contribution to atmospheric deposition are available, so this number was not included in the estimate.

Relative to a pre-urbanization scenario of land cover dominated by 100% open space, riverine TN loads increased 4-fold on a Bight-wide scale (Sengupta *et al. In Review*). Dissolved inorganic nutrients (NO_3 and NH_4) saw a disproportionately higher increase relative to organic or particulate fractions. The largest changes in the sub-regional riverine data were observed for the more heavily urbanized areas of San Pedro and Santa Monica Bay with an approximately 9-fold increase in TN and the smallest changes were observed in Ventura and Santa Barbara with a 2-fold increase in TN.

While anthropogenic changes to riverine loads are considerable, these loads still represent an order of magnitude less than effluent fluxes, the major source of anthropogenic loads to the Bight. However, total flux of nitrogen from natural sources (upwelling, atmospheric deposition and pre-urbanization rivers) was calculated and compared to the total nitrogen flux of all nutrient sources (upwelling, atmospheric deposition, post-urbanization rivers and wastewater effluent discharge). The increase in nitrogen due to anthropogenic sources was found to be largest for the Santa Monica Bay, San Pedro and San Diego sub-regions with increases of 2, 1.4, and 5.3 fold, respectively. These results are summarized in Table 7.

Table 5. Annual total nitrogen flux for each subregion (in kg N km^{-2} $year^{-1}$).

Source	Santa Barbara	Ventura	Santa Monica Bay	San Pedro	North San Diego	San Diego
Upwelling	-2.1×10^4	-1.0×10^5	1.0×10^4	2.4×10^4	3.7×10^4	2.4×10^3
Effluent	1.6×10^2	5.1×10^2	9.9×10^3	1.3×10^4	1.4×10^3	7.6×10^3
Riverine Runoff*	7.2×10^1	4.1×10^2	1.4×10^2	1.2×10^3	6.0×10^2	6.0×10^3
Atmospheric Deposition	4.3×10^2	4.3×10^2	8.7×10^2	8.7×10^2	4.3×10^2	4.3×10^2
Total Sub-regional	-2.0×10^4	-9.8×10^4	2.0×10^4	3.9×10^4	3.9×10^4	1.6×10^4

*Data for January through October 2010.

Table 6. Flux of total nitrogen for each sub-region of the SCB (in kg N km^{-2} $year^{-1}$). NA = not analyzed for this source.

Sub-Region	Total Nitrogen	Nitrate + Nitrite	Ammonia	Organic N
Santa Barbara				
Upwelling	-2.1×10^4	-1.9×10^4	-1.1×10^3	NA
Effluent	1.6×10^2	NA	1.6×10^2	NA
Riverine Runoff	7.2×10^1	9.5×10^0	3.9×10^0	5.8×10^1
Atmospheric Deposition	4.3×10^2	2.1×10^2	2.1×10^2	NA
Ventura				
Upwelling	-1.0×10^5	-9.9×10^4	-7.5×10^3	NA
Effluent	5.1×10^2	4.3×10^1	4.0×10^2	7.1×10^1
Riverine Runoff	4.1×10^2	3.5×10^2	1.7×10^1	3.8×10^1
Atmospheric Deposition	4.3×10^2	2.1×10^2	2.1×10^2	NA
Santa Monica Bay				
Upwelling	1.0×10^4	1.0×10^4	5.8×10^2	NA
Effluent	9.9×10^3	1.4×10^3	8.4×10^3	9.9×10^1
Riverine Runoff	1.4×10^2	1.1×10^1	1.1×10^1	1.3×10^2
Atmospheric Deposition	8.7×10^2	6.1×10^2	2.4×10^2	NA
San Pedro				
Upwelling	2.4×10^4	2.2×10^4	1.8×10^3	NA
Effluent	1.3×10^4	5.7×10^2	1.2×10^4	1.0×10^2
Riverine Runoff	1.2×10^3	6.3×10^2	1.0×10^2	5.0×10^2
Atmospheric Deposition	8.7×10^2	6.1×10^2	2.4×10^2	NA
North San Diego				
Upwelling	3.7×10^4	3.4×10^4	3.1×10^3	NA
Effluent	1.4×10^3	6.2×10^0	1.4×10^3	NA
Riverine Runoff	6.0×10^2	2.2×10^2	3.5×10^1	3.4×10^2
Atmospheric Deposition	4.3×10^2	2.1×10^2	2.1×10^2	NA
San Diego				
Upwelling	2.4×10^3	1.7×10^3	6.5×10^2	NA
Effluent	7.6×10^3	2.2×10^2	7.3×10^3	6.4×10^1
Riverine Runoff	6.0×10^3	1.5×10^3	3.1×10^2	4.2×10^3
Atmospheric Deposition	4.3×10^2	2.1×10^2	2.1×10^2	NA

Discussion

Importance of Anthropogenic Nutrients in Upwelling-Dominated Regions

The hypothesis that natural (upwelling) sources of nutrients contribute a substantially larger amount of nutrients to the SCB than anthropogenic sources of nutrients was tested. At the scale of the entire region, the results of this study support this hypothesis; natural sources (i.e., upwelling) dominate and anthropogenic inputs are relatively insignificant by an order of magnitude for N. However, at a sub-regional scale and proximal to the coastline (~20 km), anthropogenic N sources, particularly POTW effluent discharged to ocean outfalls, were equivalent to natural nitrogen sources in five of the six sub-regions. These findings contradict the currently held perception that in upwelling-dominated regions, anthropogenic nutrient inputs are negligible and are consistent with the growing number of studies that

Table 7. The total nitrogen flux (kg N km^{-2} $year^{-1}$) for natural nutrient sources (upwelling and atmospheric deposition) and for natural and anthropogenic sources to the SCB .

Sub-Region	Natural Sources	Natural and Anthropogenic Sources
Santa Barbara	-2.0×10^4	-2.0×10^4
Ventura	-9.9×10^4	-9.8×10^4
Santa Monica Bay	1.0×10^4	2.1×10^4
San Pedro	2.5×10^4	3.8×10^4
North San Diego	3.7×10^4	3.9×10^4
San Diego	3.0×10^3	1.6×10^4

have suggested a linkage between anthropogenic nitrogen sources and HABs in California nearshore waters (Kudela and Cochlan 2000, Kudela and Chavez 2004, Beman *et al.* 2005, Herndon and Cochlan, 2007, Howard *et al.* 2007, Cochlan *et al.* 2008, Kudela *et al.* 2008).

Importance of Temporal and Spatial Scale of Nutrient Delivery

The nutrient fluxes estimated for the four major sources in this study were calculated using annual time scales. However, it is important to recognize that nutrient delivery to the coastal ocean on shorter, daily to weekly, timescales is more ecologically relevant for primary productivity and HAB development. The timing of these nutrient sources should be considered as some sources are chronic (daily wastewater effluent discharge into oceans and into rivers), whereas other sources are seasonal (riverine runoff and upwelling). Other studies in Southern California have shown that stormwater runoff has been at times the dominant source of nitrogen inputs during non-upwelling periods and provided different proportions of nutrients than upwelling (Warrick *et al.* 2005, McPhee-Shaw *et al.* 2007). In Monterey Bay, a more extensive study of this dynamic has shown similar results where riverine inputs of nitrate exceeded upwelling inputs across short, daily to weekly, timescales, (but not monthly or annual scales), as often as 28% of days in a given year (Quay 2011).

It is important to recognize that the temporal and spatial scales used to evaluate nutrient sources will have a large impact on the results of the comparison of natural and anthropogenic sources. Similarly, the nutrient source fluxes were estimated for two spatial scales, bight-wide and local sub-regional scales. The local spatial scale is more ecologically relevant since it is similar to the scales at which algal blooms develop.

Uncertainty Associated with Nutrient Source Estimates

There was a high level of confidence in the load estimates of both TN and related constituents for riverine runoff and effluent sources. The standard error determined for riverine runoff and effluent loads was less than 20% with one exception, the riverine runoff (wet weather) ammonia (37.8) loads. Effluent loads from POTWs are monitored on a monthly basis and have been tracked over the last 30 years with a high level of quality assurance (Lyon and Stein 2008). There were insufficient data to calculate the error for the atmospheric deposition estimates, but this appears to be a very small source at the sub-regional scale. It is useful, therefore, to discuss two components of uncertainty in the nutrient source estimates: 1) modeling uncertainty and 2) inter-annual variability.

Modeling Uncertainty

In this study, a coupled hydrodynamic-biogeochemical model (ROMS/NPZD) was used to estimate upwelling. This approach produces a more accurate estimate than the more frequently used upwelling index produced by the NOAA Pacific Fisheries Environmental Laboratory (PFEL). Studies using the PFEL upwelling index typically combine the average volume over time of upwelled water with the average concentration of nitrate to estimate nitrogen flux for a specific area of coastline. For example, Warrick *et al.* (2005) calculated a nitrate upwelling flux of 2.1×10^8 kg N yr^{-1} for a 50 km section of the Santa Barbara Channel and the ICF International (2012) reports an estimate using the PFEL upwelling index of 4.3×10^8 kg N yr^{-1} (30 Km coastline) for Palos Verdes. These estimates differ from the ROMS/Biogeochemistry modeled estimate, 3.9×10^7 kg N yr^{-1} (for 50 km alongshore, 20 km offshore and 50m depth), produced by this study due to the different methodology used and inter-annual variability (see section below).

While the PFEL upwelling index characterizes large-scale atmospheric circulation patterns (Bakun 1973) and is based upon Ekman's theory of mass transport of water due to wind stress, the ROMS model is a three-dimensional, eddy-resolving physical circulation model that is able to address the variability both spatially, across a wide horizontal and vertical area and temporally, by providing highly resolved data. Therefore, the ROMS Model provided a more sophisticated method to estimate upwelling in the SCB. Additionally, due to the complex bottom topography and coastal orientation of the SCB, several published studies have concluded that the current variability within the SCB cannot be explained by wind stress (Lentz and Winant 1986, Noble *et al.* 2002, Hickey *et al.* 2003) and therefore the PFEL upwelling index is not a good representation of specific upwelling rates in southern California (Nezlin *et al.* 2012).

The coupled ROMS/NPZD model has been validated at the 15-km resolution for the entire U.S. West Coast by comparing model results with either remote sensing observations (AVHRR, SeaWiFS) or in-situ measurements from the CalCOFI Program (Gruber *et al.* 2006). While we have a high level of confidence in our results at an annual and Bight-wide scale, we must caveat our results as they become applied to seasonal or sub-regional scales. The 1-km ROMS model and NPZD used for this study has not yet been validated at this spatial scale. For this reason, it is not possible at this time to calculate the error associated with the upwelling estimates from this study. The validation of the ROMS model at 1-km resolution is on-going (but not complete as of this report), and the *in-situ* data collected during this study will be used as part of that process.

Inter-Annual Variability

The results of this study are focused on the year 2010, however, inter-annual variations in both anthropogenic and natural nutrient sources were observed. The riverine runoff has been shown by the 13-year model results to vary greatly on an inter-annual scale depending on precipitation and storm events. Figure 6 shows 2008-2009 as a relatively dry year, whereas 2009-2010 was characterized by high precipitation and resulted in 3-fold higher riverine runoff loads. Similarly, upwelling is highly variable and certainly large scale climate patterns can affect oceanographic conditions. Several ocean ecosystem indices have been developed to show changes in regional ocean conditions for the California Current System. The Pacific Decadal Oscillation (PDO) shifts every 20 to 30 years between a colder, negative phase and a warmer, positive phase. Whereas the El Niño/Southern Oscillation (ENSO) occurs about every 5 years, can last 6 to 18 months, and is characterized by variations in temperature. Indices of each of these patterns (Figures 7 and 8) show that

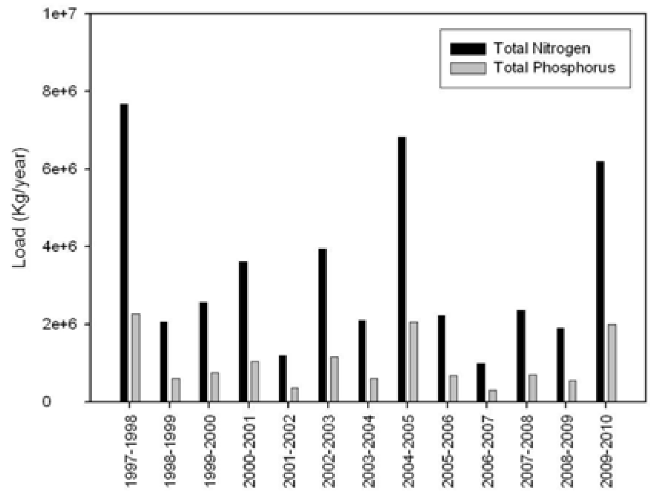

Figure 6. Total nitrogen and total phosphorus loads for the 13-year model analysis for riverine runoff.

the 2010 study period was characterized by a warm oceanographic regime (PDO), strong El Niño conditions (ENSO), and weak upwelling conditions (PFEL Upwelling Index).

The Importance of Nutrient Ratios and Forms

Nitrogen is considered to be the primary limiting macronutrient for the growth of algae in coastal waters (Dugdale 1967; Ryther and Dunstan 1971; Eppley *et al.* 1979; Nixon, 1986, 1995; Kudela and Dugdale 2000). The results from this study are consistent with previous studies in that N:P ratios calculated from the ambient nutrients measured during the ship surveys indicate nitrogen limitation in most regions.

Recent studies have shown that the form of nitrogen, not just the quantity, is important for HABs and algal blooms (Howard *et al.* 2007, Switzer 2008, Kudela *et al.* 2008, Cochlan *et al.* 2008). The sources of nitrogen to the SCB are comprised of different forms of nitrogen, mainly nitrate (plus nitrite), ammonia, and organic nitrogen (including urea). Dissolved inorganic nitrogen (DIN) was the dominant form in most natural and anthropogenic sources, except a few of the river systems, where organic nitrogen was close to equivalent (i.e., riverine runoff was 60% organic nitrogen). When we examine the forms of nitrogen that comprise each of these sources, it was surprising that effluent provides a similar nitrate (plus nitrite) load as riverine runoff to the SCB even though this form only comprises 7% of the TN load for effluent. As expected, upwelling was mostly comprised of nitrate, effluent was mostly

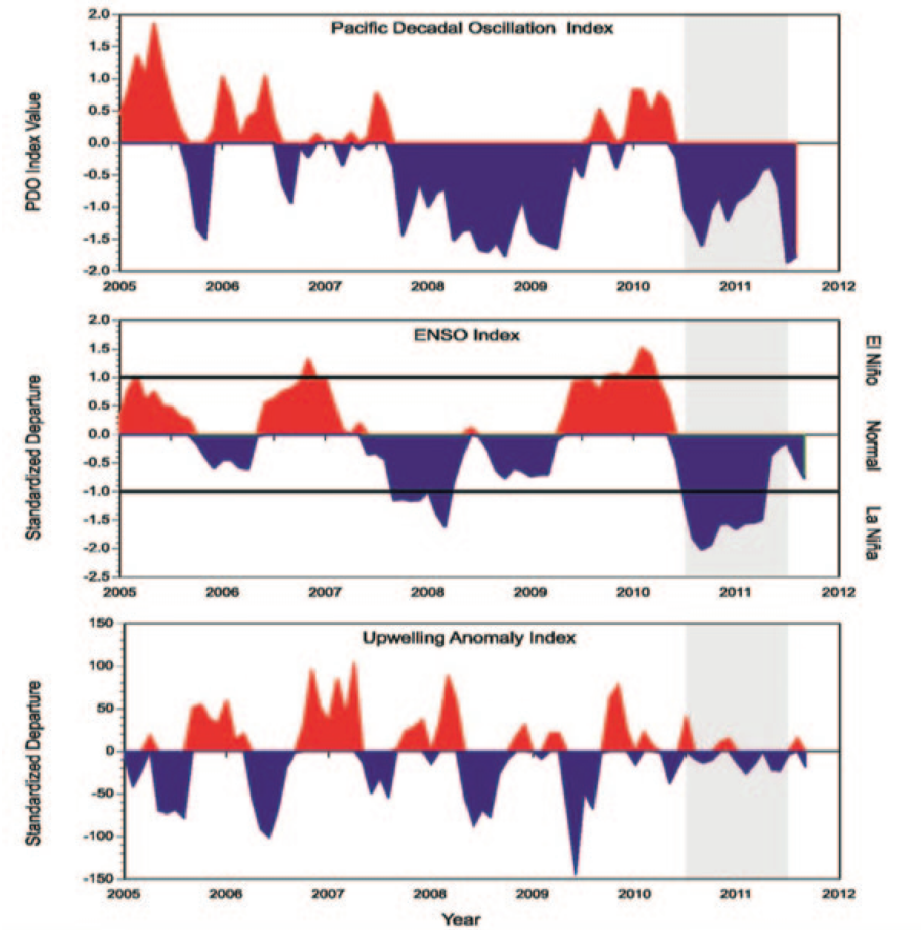

Figure 7. Ecosystem indices 2005 to 2012 for the Pacific Decadal Oscillation (PDO) Index, the El Niño/Southern Oscillation (ENSO) Index, and the PFEL Upwelling Anomality Index (from the Orange County Sanitation District Annual Report 2011).

comprised of ammonia, and riverine runoff was comprised of a mixture of inorganic and organic nitrogen forms. Organic nitrogen was mostly derived from riverine runoff (60% on a bight-wide scale).

Urea, an organic nitrogen form used as an indicator of coastal runoff (Kudela and Cochlan 2000) has been found to sustain HABs in central and southern California, and California HAB species have been shown to utilize urea for growth (McCarthay 1972, Eppley *et al.* 1979, Kudela and Cochlan 2000, Herndon and Cochlan 2007, Howard *et al.* 2007, Cochlan *et al.* 2008, Kudela *et al.* 2008). Despite these studies, urea concentrations in California's coastal waters and the importance of urea as a nitrogen source for algal growth is often overlooked and understudied. The main source of urea to the SCB was determined to be riverine runoff as urea comprised 1% or less of the large POTW effluent loads.

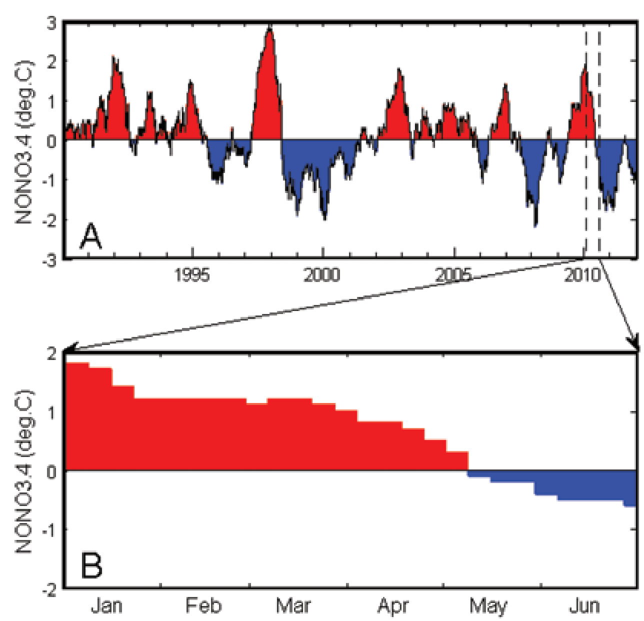

Figure 8. El Nino index (NINO3.4 is sea surface temperature anomaly in the equatorial Pacific region 5°N–5°S:170–120°W) during 1990-2011 (A) and January-June 2010 (B).

Future studies are needed to determine the amount of biological productivity that is attributable to anthropogenic nutrient sources in the SCB. A multi-year source analysis should be conducted in order to determine inter-annual variability for each source. Additional studies are needed in order to provide a sufficient amount of atmospheric deposition-rate data for a multi-year analysis and to further investigate atmospheric deposition as a nutrient source in coastal waters. The models used in this study can be used to conduct a multi-year source comparison using the ROMS model coupled with the NPDZ model to determine inter-annual variability among sources. These models can also be used to assess various nutrient source scenarios and to determine the biological productivity that results from anthropogenic nutrients.

Summary

At a regional, bight-wide scale, natural nutrient sources make a much larger contribution of nutrients than anthropogenic sources. At smaller sub-regional spatial scales, which are more ecologically relevant to the development of algal blooms, the quantity of anthropogenic and natural nitrogen sources are comparable in orders of magnitude. The anthropogenic nutrient sources were mostly comprised of dissolved inorganic nitrogen. The organic nitrogen was only evaluated in two sources (riverine runoff and effluent) and the riverine runoff was the main source of organic nitrogen to the SCB. Urea was a measurable source of nitrogen in the SCB but a minor component of the overall nitrogen load. These results suggest that the spatial scale used in the analysis will affect the relative comparison between anthropogenic and natural nutrient sources. While this study was designed to be a first order estimation of nutrient sources, the results suggest that anthropogenic nutrients are significant at spatial scales relevant to algal bloom development.

Literature Cited

D. Ackerman and K. Schiff. 2003. Modeling stormwater mass emissions to the southern California Bight. *Journal of the American Society of Civil Engineers* 129:308-323.

Anderson, D.M., P.M. Glibert and J.M. Burkholder. 2002. Harmful algal blooms and eutrophication: Nutrient sources, composition, and consequences. *Estuaries* 25:704-726.

Anderson, D.M., J.M. Burkholder, W.P. Cochlan, P.M. Glibert, C.J. Gobler, C.A. Heil, R.M. Kudela, M.L. Parsons, J.E. Rensel, D.W. Townsend, V.L. Trainer and G.A. Vargo. 2008. Harmful algal blooms and eutrophication: Examining linkages from selected coastal regions of the United States. *Harmful Algae* 8:39-53.

Bakun, A. 1973. Coastal upwelling indices, west coast of North America, 1946–1971. National Oceanic and Atmospheric Administration (NOAA) Technical Report NMFS SSRF-671. UnitedStates Department of Commerce. Washington, DC.

Beman, M., K. Arrigo and P. Matson. 2005. Agricultural runoff fuels large phytoplankton blooms in vulnerable areas of the ocean. *Nature* 434:211-214.

Bray, N.A., A. Keyes and W.M. Morawitz. 1999. The California Current system in the Southern California Bight and the Santa Barbara Channel. *Journal of Geophysical Research-Oceans* 104:7695-7714.

Brzezinski, M.A. 1985. The Si:C:N ratio of marine diatoms: interspecific variability and the effect of some environmental variables. *Journal of Phycology* 21:347-357.

Burkov, V.A. and Y.V. Pavlova. 1980. Description of the eddy field of the California Current. *Oceanology. English Translation* 20:272-278.

Busse, L.B., E.L. Venrick, R. Antrobus, P.E. Miller, V. Vigilant, M.W. Silver, C. Mengelt, L. Mydlarz and B.B. Prezelin. 2006. Domoic acid in phytoplankton and fish in San Diego, CA, USA. *Harmful Algae* 5:91-101.

Caron, D.A., M.E. Garneau, E. Seubert, M.D. Howard, L. Darjany, A. Schnetzer, I. Cetinic, G. Filteau, P. Lauri, B. Jones and S. Trussell. 2010. Harmful algae and their potential impacts on desalination operations off southern California. *Journal of Water Research* 44:385-416.

Chisholm, J.R., F.E. Fernex, D. Mathieu and J.M. Jaubert. 1997. Wastewater discharge, seagrass decline and algal proliferation on the Cote d' Azur. *Marine Pollution Bulletin* 34:78-84.

Cochlan, W.P., J. Herndon and R.M. Kudela. 2008. Inorganic and organic nitrogen uptake by the toxigenic diatom *Pseudo-nitzschia australis* (Bacillariophyceae). *Harmful Algae* 8:111-118.

Dailey, M.D., J.W. Anderson, D.J. Reish and D.S. Gorsline. 1993. The Southern California Bight: background and setting. pp. 1-18 *in*: M.D. Dailey, D.J. Reish and J.W. Anderson (eds.), Ecology of the Southern California Bight. University of California Press. Berkeley, CA.

Dong, C., E.Y. Idica and J.C. McWilliams. 2009. Circulation and multiple-scale variability in the Southern California Bight. *Progress in Oceanography* 82:168-190.

Dorman, C.E. and C.D. Winant. 1995. Buoy observations of the atmosphere along the west coast of the United States. *Journal of Geophysical Research-Oceans* 100:16029-16044.

Dugdale, R.C. 1967. Nutrient limitation in the sea: Dynamics, identification and significance. *Limnology Oceanography* 12:685-695.

Emery, K.O. 1960. The Sea Off Southern California. John Wiley and Sons. New York, NY.

Eppley, R., E. Renger and W. Harrison. 1979. Nitrate and phytoplankton production in California coastal waters. *Limnology and Oceanography* 24:483-494.

GEOHAB. 2006. Global ecology and oceanography of harmful algal blooms. *Harmful Algal Blooms in Eutrophic Systems* 74.

Glibert, P.M., D.M. Anderson, P. Gentien, E. Granéli and K.G. Sellner. 2005a. The global, complex phenomena of harmful algal blooms. *Oceanography* 18:137-147.

Glibert, P.M., S. Seitzinger, C.A. Heil, J.M. Burkholder, M.W. Parrow, L.A. Codispoti and V. Kelly. 2005b. The role of eutrophication in the global proliferation of harmful algal blooms. *Oceanography* 18:198-209.

Glibert, P.M., J. Harrison, C. Heil and S. Seitzinger. 2006. Escalating worldwide use of urea - a global change contributing to coastal eutrophication. *Biogeochemistry* 77:441-463.

Greenberg, A.E., L.S. Clesceri and A.D. Eaton. 1992. Standard Methods for the Examination of Water and Wastewater, 18th edition. American Public Health Association. Washington, DC.

Gruber, N., H. Frenzel, S.C. Doney, P. Marchesiello, J.C. McWilliams, J.R. Moisan, J.J. Oram, G.K. Plattner and K.D. Stolzenbach. 2006. Eddy-resolving simulation of plankton ecosystem dynamics in the California Current System. *Deep Sea Research I* 53:1483-1516.

Gruber, N., Z. Lachkar, H. Frenzel, P. Marchesiello, M. Münnich, J.C. McWilliams, T. Nagai, and G.K. Plattner. 2011. Eddy-induced reduction of biological production in eastern boundary upwelling systems. *Nature Geoscience* 4:787-792.

Hallegraeff, G.M. 1993. A review of harmful algal blooms and their apparent global increase. *Phycologia* 32:79-99.

Hallegraeff, G.M. 2004. Harmful algal blooms: A global overview. pp. 25-49 *in:* G.M. Hallegraeff, D.M. Anderson and A.D. Cembella (eds.), Manual on Harmful Marine Microalgae. UNESCO. Paris, France.

Haney, R.L., R.A. Hale and D.E. Dietrich. 2001. Offshore propagation of eddy kinetic energy in the California Current. *Journal of Geophysical Research-Oceans* 106:11709-11717.

Hamilton, P., M.A. Noble, J. Largierc, L.K. Rosenfeldd and G. Robertsone. 2006. Cross-shelf subtidal variability in San Pedro Bay during summer. *Continental Shelf Research* 26:681-702.

Harms, S. and C.D. Winant. 1998. Characteristic patterns of the circulation in the Santa Barbara Channel. *Journal of Geophysical Research-Oceans* 103:3041-3065.

Heisler, J., P. Glibert, J. Burkholder, D. Anderson, W. Cochlan, W. Dennison, C. Gobler, Q. Dortch, C. Heil, E. Humphries, A. Lewitus, R. Magnien, H. Marshall, K. Sellner, D. Stockwell, D. Stoecker and M. Suddleson. 2008. Eutrophication and harmful algal blooms: A scientific consensus. *Harmful Algae* 8:3-13.

Herndon, J. and W.P. Cochlan. 2007. Nitrogen utilization by the raphidophyte *Heterosigma akashiwo*: Growth and uptake kinetics in laboratory cultures. *Harmful Algae* 6:260-270.

Hickey, B.M. 1979. The California Current system: Hypotheses and facts. *Progress in Oceanography* 8:191-279.

Hickey, B.M. 1992. Circulation over the Santa Monica-San Pedro basin and shelf. *Progress in Oceanography* 30:37-115.

Hickey, B.M., E.L. Dobbins and S.E. Allen. 2003. Local and remote forcing of currents and temperature in the central Southern California Bight. *Journal Phytoplankton blooms detected by SeaWiFS* - 320 *of Geophysical Research-Oceans* 108:3081, doi:3010.1029/2000JC000313.

Howard, M.D., W.P. Cochlan, R.M. Kudela and N. Ladizinsky. 2007. Nitrogenous preference of toxic *Pseudo-nitzschia australis* (Bacillariophyceae) from field and laboratory experiments. *Harmful Algae* 6:206-217.

Howarth, R.W. 2008. Coastal nitrogen pollution: a review of sources and trends globally and regionally. *Harmful Algae* 8:14-20.

Howarth, R.W., D. Walker and A. Sharpley. 2002a. Sources of nitrogen pollution to coastal waters of the United States. *Estuaries* 25:656-676.

Howarth, R.W., E.W. Boyer, W.J. Pabich and J.N. Galloway. 2002b. Nitrogen use in the United States from 1961 to 2000 and potential future trends. *Ambio* 31:88-96.

ICF International. 2012. Preliminary Screening Analysis for the Clearwater Program. (ICF 00016.07.) Prepared for the Sanitation Districts of Los Angeles County. Irvine, CA.

Jaubert, J.M., R.J. Chisholm, A. Minghelli-Roman, M. Marchioretti, J.H. Morrow and H.T. Ripley. 2003. Re-evaluation of the extent of *Caulerpa taxifolia* development in the northern Mediterranean using airborne spectrographic sensing. *Marine Ecology Progress Series* 263:75-82.

Kudela, R. and R. Dugdale. 2000. Nutrient regulation of phytoplankton productivity in Monterey Bay, California. *Deep-Sea Research II* 47:1023-1053.

Kudela, R.M. and W.P. Cochlan. 2000. The kinetics of nitrogen and carbon uptake and the influence of irradiance for a natural population of *Lingulodinium polyedrum* (Pyrrophyta) off southern California. *Aquatic Microbial Ecology* 21:31-47.

Kudela, R.M. and F.P. Chavez. 2004. The impact of coastal runoff on ocean color during an El Nino year in central California. *Deep Sea Research* 51:1173-1185.

Kudela, R.M., J.Q. Lane and W.P. Cochlan. 2008. The potential role of anthropogenically derived nitrogen in the growth of harmful algae in California, USA. *Harmful Algae* 8:103-110.

Lange, C.B., F.M. Reid and M. Vernet. 1994. Temporal distribution of the potentially toxic diatom *Pseudo-nitzschia australis* at a coastal site in southern California. *Marine Ecology Progress Series* 104:309-312.

Lapointe, B.E. 1997. Nutrient thresholds for bottom-up control of macroalgal blooms on coral reefs in Jamaica and southeast Florida. *Limnology and Oceanography* 42:1119-1131.

Lapointe, B.E., P.J. Barile, M.J. Wynne and C.S. Yentsch. 2005a. Reciprocal invasion: Mediterranean native *Caulerpa ollivieri* in the Bahamas supported by human nitrogen enrichment. *Aquatic Invaders* 16:2-5.

Lapointe, B., P.J. Barile, M.M. Littler and D.S. Littler. 2005b. Macroalgal blooms on southeast Florida coral reefs II. Cross-shelf discrimination of nitrogen sources indicates widespread assimilation of sewage nitrogen. *Harmful Algae* 4:1106-1122.

Lapointe, B.E., P.J. Barile and W.R. Matzie. 2004. Anthropogenic nutrient enrichment of seagrass and coral reef communities in the lower Florida keys: Discrimination of local versus regional nitrogen sources. *Journal of Experimental Marine Biology and Ecology* 308:23-58.

Lentz, S.J. and C.D. Winant. 1986. Subinertial currents on the southern California shelf. *Journal of Physical Oceanography* 16:1737-1750.

Lynn, R.J. and J.J. Simpson. 1987. The California Current System: The seasonal variability of its physical characteristics. *Journal of Geophysical Research-Oceans* 92:12947-12966.

Lyon, G.S. and E.D. Stein. 2008. Effluent discharges to the Southern California Bight from small municipal wastewater treatment facilities in 2005. pp. 1-14 *in*: S.B. Weisberg and K. Miller (eds.), Southern California Coastal Water Research Project 2008 Annual Report. Costa Mesa, CA.

Marchesiello, P., J.C. McWilliams and A.F. Shchepetkin. 2003. Equilibrium structure and dynamics of the California Current system. *Journal of Physical Oceanography* 33:753-783.

McCarthy, J.J. 1972. The uptake of urea by natural populations of marine phytoplankton. *Limnology and Oceanography* 17:738-748.

McPhee-Shaw, E.E., D.A. Siegel, L. Washburn, M.A. Brzezinski, J.L. Jones, A. Leydecker and J. Melack. 2007. Mechanisms for nutrient delivery to the inner shelf: Observations from the Santa Barbara Channel. *Limnology and Oceanography* 52:1748-1766.

Moumen, N., S.-M. Yi, H.A. Raymond, Y.J. Han and T.M. Holsen. 2004. Quantifying the dry deposition of ammonia in ammonia-rich and ammonia-poor environments using a surrogate surface approach. *Atmospheric Environment* 38:2677-2686.

Nixon, S.W. 1986. Marine end environmental pollution. pp. 97-11 *in*: R. Halwagy, D. Clayton and M. Behbehani (eds.), Nutrient Dynamics and the Productivity of Marine Coastal Waters. Alden Press. Oxford, UK.

Nixon, S.W. 1995 . Coastal marine eturophication: A definition, social causes, and future concerns. *Ophelia* 41:199-219.

Nezlin, N.P., M.A. Sutula, R.P. Stumpf and A. Sengupta. 2012. Phytoplankton blooms detected by SeaWiFS along the central and southern California Coast. *Journal of Geophysical Research* 117:C07004.

Noble, M.A., H.F. Ryan and P.L. Wiberg. 2002. The dynamics of subtidal poleward flows over a narrow continental shelf, Palos Verdes, CA. *Continental Shelf Research* 22:923-944.

O'Loughlin, G., W. Huber and B. Chocat. 1996. Rainfall-runoff processes and modeling. *Journal of Hydraulic Research* 34:733-751.

Paerl, H.W. and M.F. Piehler. 2008. Nitrogen and marine eutrophication. pp. 529-567 *in*: D. Capone, D. Bronk, M. Mulholland and E. Carpenter (eds.). Nitrogen in the Marine Environment, 2nd edition. Elsevier. Burlington, MA.

Quay, J. 2011. New Tools and Insight for the Recognition of *Pseudo-nitzschia* blooms and Toxin Incidence. PhD Dissertation: Ocean Science. University of California. Santa Cruz, CA.

Raymond, H.A, S.-M. Yi, N. Moumen, Y.J. Han and T.M. Holsen. 2004. Quantifying the dry deposition of reactive nitrogen and sulfur containing species in remote areas using a surrogate surface analysis approach *Atmospheric Environment* 38:2687-2697

Reid Jr., J.L. and A.W. Mantyla. 1976. The effect of the geostrophic flow upon coastal sea elevations in the northern North Pacific ocean. *Journal of Geophysical Research* 81:3100-3110.

Ryther, J. and W. Dunstan. 1971. Nitrogen, phosphorus and eutrophication in the coastal marine environment. *Science* 171:1008-1112.

Sabin, L.D. and K.C. Schiff. 2008. Dry atmospheric deposition rates of metals along a coastal transect in southern California. *Atmospheric Environment* 42:6606-6613.

Sengupta, A., M.A. Sutula, K. McLaughlin, M.D. Howard, L. Tiefenthaler, T. VonBitner, F.A. Gonzalez and A. Anslem. *In Review*. Riverine nutrient loads and fluxes to the Southern California Bight (USA). *Estuaries and Coasts*.

Shchepetkin, A.F. and J.C. McWilliams. 2005. The regional oceanic modeling system (ROMS): A split-explicit, free-surface, topography-following-coordinate oceanic model. *Ocean Modeling* 9:347-404.

Shchepetkin, A.F. and J.C. McWilliams. 2008. Computational kernel algorithms for fine-scale, multi-process, long-term oceanic simulations. pp. 121-186 *in*: R. Temam and J. Tribbia (eds.), Handbook of Numerical Analysis: Computational Methods for the Ocean and the Atmosphere. Elsevier. Oxford, UK.

Smayda, T.J. 1990. Novel and nuisance phyto-plankton blooms in the sea: evidence for a global epidemic. pp. 29-40 i*n:* E. Granéli, B. Gundström, L. Edler and D.M. Anderson (eds.), Toxic Marine Phytoplankton. Elsevier. New York, NY.

Strub, P.T. and C. James. 2000. Altimeter-derived variability of surface velocities in the California Current System: 2. Seasonal circulation and eddy statistics. *Deep-Sea Research II* 47:831-870.

Sverdrup, H.U. and R.H. Fleming. 1941. The waters off the coast of southern California, March to July 1937. *Bulletin of the Scripps Institution of Oceanography* 4:261-378.

Switzer, T. 2008. Urea loading from a spring storm - Knysna estuary, South Africa. *Harmful Algae* 8:66-69.

Thompson, P. and A. Waite. 2003. Phytoplankton responses to wastewater discharges at two sites in Western Australia. *Marine and Freshwater Research* 54:721-735.

Warrick, J., L. Washburn, M. Brzezinski and D. Siegel. 2005. Nutrient contributions to the Santa Barbara Channel, California, from the ephemeral Santa Clara River. *Estuarine, Coastal and Shelf Science* 62:559-574.

Acknowledgements

This research was supported by funding provided by the California Ocean Protection Council (Grant Agreement No. 08-095) and the State Water Resources Control Board (Agreement No. 08-060-250). The authors also wish to express their gratitude to Becky Schaffner for assistance with map preparation and to sampling personnel from the following organizations: City of San Diego, Orange County Sanitation District, Los Angeles County Sanitation District, City of Los Angeles, Southern California Coastal Water Research Project, Aquatic Bioassay and Consulting Laboratories.